Amino Acids (2014) 46:2615–2625
DOI 10.1007/s00726-014-1805-0

ORIGINAL ARTICLE

The functional role of Cys3–Cys4 loop in hydrophobin HGFI

Baolong Niu · Yanbo Gong · Xianghua Gao · Haijin Xu · Mingqiang Qiao · Wenfeng Li

Received: 4 January 2014 / Accepted: 3 July 2014 / Published online: 21 September 2014

Abstract Hydrophobins are a large group of low-molecular weight proteins. These proteins are highly surface-active and can form amphipathic membranes by self-assembling at hydrophobic–hydrophilic interfaces. Based on physical properties and hydropathy profiles, hydrophobins are divided into two classes. Upon the analysis of amino acid sequences and higher structures, some models suggest that the Cys3–Cys4 loop regions in class I and II hydrophobins can exhibit remarkable difference in their alignment and conformation, and have a critical role in the rodlets structure formation. To examine the requirement for the Cys3–Cys4 loop in class I hydrophobins, we used protein fusion technology to obtain a mutant protein HGFI-AR by replacing the amino acids between Cys3 and Cys4 of the class I hydrophobin HGFI from *Grifola frondosa* with those ones between Cys3 and Cys4 of the class II hydrophobin HFBI from *Trichoderma reesei*. The gene of the mutant protein HGFI-AR was successfully expressed in *Pichia pastoris*. Water contact angle (WCA) and X-ray photoelectron spectroscopy (XPS) measurements demonstrated that the purified HGFI-AR could form amphipathic membranes by self-assembling at mica and hydrophobic polystyrene surfaces. This property enabled them to alter the surface wettabilities of polystyrene and mica and change the elemental composition of siliconized glass. In comparison to recombinant class I hydrophobin HGFI (rHGFI), the membranes formed on hydrophobic surfaces by HGFI-AR were not robust enough to resist 1 % hot SDS washing. Atomic force microscopy (AFM) measurements indicated that unlike rHGFI, no rodlet structure was observed on the mutant protein HGFI-AR coated mica surface. In addition, when compared to rHGFI, no secondary structural change was detected by Circular Dichroism (CD) spectroscopy after HGFI-AR self-assembled at the water–air interface. HGFI-AR could not either be deemed responsible for the fluorescence intensity increase of Thioflavin T (THT) and the Congo Red (CR) absorption spectra shift (after the THT(CR)/HGFI-AR mixed aqueous solution was drastically vortexed). Remarkably, replacement of the Cys3–Cys4 loop could impair the rodlet formation of the class I hydrophobin HGFI. So, it could be speculated that the Cys3–Cys4 loop plays an important role in conformation and functionality, when the class I hydrophobin HGFI self-assembles at hydrophobic–hydrophilic interfaces.

Keywords Hydrophobin · HGFI · Self-assembly · Cys3–Cys4 loop · Rodlets structure

B. Niu · X. Gao · W. Li (✉)
Key Laboratory of Interface Science and Engineering in Advanced Materials, College of Materials Science and Engineering, Taiyuan University of Technology, Ministry of Education, Taiyuan 030024, People's Republic of China
e-mail: wenfenglityut@live.com

B. Niu · X. Gao · W. Li
College of Materials Science and Engineering, Taiyuan University of Technology, Taiyuan 030024, People's Republic of China

Y. Gong
College of Light Textile Engineering and Art, Taiyuan University of Technology, Taiyuan 030024, People's Republic of China

H. Xu · M. Qiao
State Key Laboratory of Medicinal Chemical Biology, College of Life Sciences, Nankai University, No. 94 Weijin Road, Tianjin 300071, People's Republic of China
e-mail: Mingqiangqiao@live.com

Introduction

Hydrophobins are a large family of small secreted proteins that are solely produced by filamentous fungi (Morris et al.

2011; Hakanpää et al. 2004; Wessels et al. 1991). These proteins fulfill a wide variety of functions in fungal growth, development and pathogenesis (Wessels 1996; Wösten and Wessels 1997; Wösten 2001). For instance, they mediate the emergence of aerial hyphae by reducing the surface tension which allows them to escape from the aqueous environment (Wösten et al. 1999). They also can facilitate the adhesion of conidiospores to host surfaces (Talbot et al. 1996; Ma et al. 2006) and gas exchange in fruiting bodies through forming hydrophobic air channels (Lugones et al. 1998; Trembley et al. 2002).

Although the amino acid sequence and composition are diverse among hydrophobins, there is a main unifying feature that all of them possess eight conserved cysteine residues that form four intramolecular disulfide bonds (Hakanpää et al. 2006; Kershaw and Talbot 1998). According to their hydropathy pattern and biophysical properties, hydrophobins are classified into two classes, I and II (Wessels 1994; de Vries et al. 1999). Both classes of hydrophobins can self-assemble at hydrophilic–hydrophobic interfaces into amphipathic films (Linder 2009).

The class I hydrophobins are poorly soluble even under conditions such as in 2 % boiling SDS, and can be solubilized only by treatment with solvents such as 100 % trifluoroacetic acid (TFA) and formic acid (Butko et al. 2001). Meanwhile, rodlets are typically observed by electron microscopy or atomic force microscopy (AFM) when dilute class I hydrophobin solution drips and dries down on a solid support (Sunde et al. 2008; Wang et al. 2010b; Yu et al. 2008; Houmadi et al. 2008; Basheva et al. 2011). Unlike the class I hydrophobin, the membranes formed by assembled class II proteins can be dissociated under mild conditions (such as 60 % ethanol or 2 % SDS) (Yang et al. 2013). Moreover, no rodlets are observed when dilute class II hydrophobin solutions drip and dry down on a solid support (Scholtmeijer et al. 2001). But the membranes formed by class II hydrophobins imaged by AFM show an organized structure when the dilute solutions drip and dry down onto a mica support (Sbrana et al. 2010). Circular dichroism (CD) shows that the class I hydrophobins contain substantial amount of β-sheet structure in the soluble state and a significant secondary structural changes appear after vortexing the aqueous solution (de Vocht et al. 1998). While, except for a slight alteration of intensity, no changes in the CD spectra of class II hydrophobins were observed after vigorous vortexing the solutions (Wösten and de Vocht 2000).

In our previous study, we observed that like other class I hydrophobins, HGFI from *Grifola frondosa* could self-assemble into amyloid-like rodlets on mica and polystyrene surfaces (Yu et al. 2008; Wang et al. 2010b). The class I hydrophobin HGFI membrane formed on the polystyrene surface was extremely robust against washing and could even resist hot SDS treatments (Hou et al. 2009).

The class II hydrophobins HFBI from *Trichoderma reesei* could also form aggregates at water–air interfaces; however, they were of less regular shape and more unstable (Serimaa et al. 2003; Paananen et al. 2003). The membranes formed by the class II hydrophobin HFBI on Teflon surfaces could resist aqueous washes but not treatment with hot SDS (Askolin et al. 2006). In addition and unlike the class I hydrophobins, HFBI could not react with the stain ThT and cause the fluorescence intensity of the mixture to increase. Circular dichroism (CD) showed that class I hydrophobins exhibited a predominant β-sheet structure indicated by the minima at 214–217 nm when β-sheet structure was induced by vortexing the aqueous solution (Wösten and de Vocht 2000; Ma et al. 2008; Paslay et al. 2013). It should be noticed that the structural changes of class II hydrophobins at the air–water interface were not observed due to instability of the assemblages (Askolin et al. 2006; Wösten and de Vocht 2000; Paslay et al. 2013).

There is little available information about the three-dimensional structure and the rodlets' assembly mechanism of class I hydrophobin HGFI. It was shown that the second loop formed by the amino acid residues between the third Cys (Cys3) and the fourth Cys (Cys4) of class I hydrophobins played a pivotal role in self-assembly at the hydrophilic–hydrophobic interface (Wang et al. 2004). Moreover, the model proposed for the polymeric rodlet structure formation of the hydrophobin EAS also suggested that the second loop of class I hydrophobins played an important role in the initial formation of self-assembled structures at a hydrophilic–hydrophobic interface (Kwan et al. 2006). However, it was demonstrated that the Cys3–Cys4 loop did not have an integral role in the formation or structure of the EAS rodlets (Kwan et al. 2008). Unlike the class I hydrophobins, in class II hydrophobin HFBI, the loop formed by the amino acid residues between Cys3 and Cys4 is much smaller and the number is conserved in all class II hydrophobins (Linder et al. 2005).

Therefore, to study the influence of Cys3–Cys4 loop on self-assembly and rodlets structure formation in HGFI, we used protein fusion technology to obtain a mutant protein HGFI-AR by replacing the Cys3–Cys4 loop of HGFI with the loop that is present in the typical class II hydrophobin HFBI, and investigated its properties.

Materials and methods

Strains, vectors and reagents

Escherichia coli (*E. coli*) strain DH5a, *Pichia pastoris* (*P. pastoris*) strain GS115 ($His^{-}Mut^{-}$), and the pPIC9 vector were purchased from Invitrogen (Beijing, China). The recombinant class I hydrophobin HGFI (rHGFI),

Table 1 Primers used in the current study

Name	Sequence 5′–3′
P1	CGCTCGAG***AAAAGA***CAACAGTGCACCACTGGC
P2	**GTCAAGGCCGATGAGGCCAAGGACTTGGGTGGC**GCAGCACTGGAGCTG
P3	**GCCACCCAAGTCCTTGGCCTCATCGGCCTTGAC**TGCTCGCCGATCTCC
P4	CGGAATTCAGACGTTAACCGGAACAC
5′AOX	GACTGGTTCCAATTGACAAGC
3′AOX	GCAAATGGCATTCTGACATCC

The restriction sites and Kex2 protease cleavage site are in underline and bolditalics, respectively; the 33-bp gene fragment encoding the amino acid sequence between Cys3 and Cys4 of HFBI and the reversed complementary sequence are in bold

pMD19-T-*hfbI*, and pET-28a-*hgfI* were provided by our laboratory. All restriction enzymes, Taq DNA polymerase, T4 DNA ligase and pMD19-T vector were purchased from TaKaRa (Dalian, China). DNA fragment purification kits, DNA markers and protein markers were supplied by TaKaRa (Dalian, China). All primers were also synthesized by Takara. Other chemicals and reagents were purchased either from TaKaRa or Sigma.

Vector construction

A three-step procedure was used to obtain *hgfI-ar* gene by PCR. First, to obtain gene A1, a pET-28a-*hgfI* vector containing a class I hydrophobin gene *hgfI* from *G. frondosa* was used as a template, and P1/P2 were used as forward and reserves primers, respectively. The sequences of the primers used are shown in Table 1. The KEX2 protease cleavage site following the *Xho*I restriction site was inserted at the 5′-terminal of P1, and a 33 bp gene fragment encoding the amino acid sequence between Cys3 and Cys4 of HFBI was added to the 5′ end of P2.

Second, a pMD19-T-*hfbI* vector containing the class II hydrophobin HFBI from *Trichoderma reesei* was used as a template and P3/P4 as forward/reserves primers to obtain gene A2. A 33-bp gene sequence reversed complementary with the one added to the 5′ end of P2 was added to the 5′ end of P3, and an *Eco*RI restriction site sequence was added to the 5′ end of P4.

Third, the *hgfI-ar* coding sequence which contained an *Xho*I restriction site and Kex2 protease cleavage site at 5′ end and an *Eco*RI restriction site at 3′ end was amplified by PCR using the A1 and A2 together as templates and P1/P4 as forward/reserves primers. Then, they were cloned into pMD19-T. The recombinant plasmid was transformed into *E. coli* DH5α and the plasmids containing the insert *hgfI-ar* coding sequence were verified by both double-enzyme (*Xho*I and *Eco*RI) cleavage method and sequencing. The *hgfI-ar* gene in pMD19-T was then subcloned into the pPIC9 vector using the engineered *Xho*I and *Eco*RI sites, yielding pPIC9-*hgfI-ar*. In the recombinant pPIC9-*hgfI-ar* vector, the *hgfI-ar* gene was located downstream from the AOX1 promoter, which can be induced using methanol as sole carbon source. To ensure secretion of HGFI-AR, the α-factor secretion signal was placed upstream of the expressing gene and the final recombinant vector pPIC9-*hgfI-ar* was verified by the *Xho*I and *Eco*RI cleavage and gene sequence analysis using primer pairs 5′ AOX/3′ AOX.

Transformation and expression

The plasmid pPIC9-*hgfI-ar* was linearized with *Stu*I, and transfected into *P. pastoris* GS115 (His^-) cells by electroporation using a Bio-Rad gene pulser apparatus (25μF, 200 Ω, 2.0 kV) according to the manufacturer's instructions. Transformants were plated on minimal dextrose (MD) medium to screen for the His^+ clones. Fifty His^+ clones were selected and subsequently patched on MD and minimal methanol (MM) plates to determine the His^+ Mut^+ phenotypes. Colony PCR and sequencing were performed using the primers 5′AOX1 and 3′AOX1 to confirm the integration of *hgfI-ar* into the *P. pastoris* genome. The positive clones were chosen for future work.

Fermentation and purification of recombinant HGFI-AR

The selected fast-growing strains (His^+ Mut^+) were incubated in 50 mL buffered minimal glycerol (BMG) medium and cultured at 30 °C and 250 rpm until the OD_{600} reached 6. The cells were then harvested by centrifugation for 30 min at 8,000*g* and resuspended in 100 mL buffered minimal methanol (BMM) medium and cultured at 28 °C and 250 rpm. The expression of HGFI-AR was induced by methanol supplementation to a final concentration of 0.5 % at 24 h intervals for 5 days. The supernatants were gathered for purification and analysis of the recombinant protein HGFI-AR. The expression levels of HGFI-AR from the 10 clones were analyzed by Tricine–SDS-PAGE, and the clone that expressed the highest level of HGFI-AR was chosen for large-scale production following the procedure reported previously (Niu et al. 2012b). After 96 h of induction time,

the culture was centrifuged at 8,000*g* to obtain the supernatant. A two-step process was used to purify the protein HGFI-AR (Wang et al. 2010a). The first step was ultrafiltration using a hollow fiber membrane module with 4 kDa molecular weight cut-off (Tianjin MOTIMO Membrane Technology Ltd., China) and then lyophilized. RP-HPLC was used to further purify the protein HGFI-AR with a Vydac C4 reversed-phase column (4.6 × 250 mm, GRACE, China) (Yu et al. 2008). The purified HGFI-AR was identified by 16 % Tricine–SDS-PAGE, Western blotting and mass spectra.

Water contact angle (WCA) measurements

The surfaces of hydrophobic polystyrene and hydrophilic mica coated with purified HGFI-AR were analyzed using WCA measurements. 20 μL of 0.02 mg/mL protein solution was used to coat the polystyrene (25 mm × 25 mm) and mica surfaces (25 mm × 25 mm). After incubating at room temperature for 30 min, the solution was removed gently and the modified polystyrene and mica surfaces were dried under a nitrogen stream. The surfaces were kept at room temperature overnight. WCA measurements of unmodified and HGFI-AR-modified polystyrene surfaces were performed after rinsing with water or 1 % hot SDS. WCA measurements of unmodified and HGFI-AR-modified mica surfaces were also carried out after rinsing them with water or 1 % hot SDS. WCAs were measured with a 5μL of water droplet on the modified and unmodified surfaces using an optical contact angle meter (Kruss, DSA100) at room temperature. The average values of WCA measurements were obtained from three water droplet readings at different locations.

X-ray photoelectron spectroscopy (XPS) measurements

HGFI-AR sample at a concentration of 100 μg/ml in Milli-Q™ water (MQW) was used. The elemental composition of bare and HGFI-AR coated siliconized glasses was analyzed by XPS (Kratos Axis Ultra DLD) spectrometer employing a monochromated Al–Ka X-ray radiation source (hv = 1486.6 eV), hybrid (magnetic/electrostatic) optics and a multi-channel plate and delay line detector (DLD). All XPS spectra were recorded using an aperture slot of 300 × 700 μm. The survey spectra were recorded with a pass energy of 160 eV, and high-resolution spectra with a pass energy of 40 eV.

Atomic force microscope (AFM) measurements

Tapping mode images of dried droplets were obtained using a NanoScope IIIa Multimode atomic force microscope (Veeco Instruments, NY, USA) and silicon nitride cantilevers with a nominal force constant of 50 N/m. Scan rates were approximately 1 Hz. The damping ratio (set-point amplitude/free amplitude) was typically about 0.7–0.8. The Scanning Probe Image Processor (SPIP; Image Metrology, Lyngby, Denmark) was used for image analysis. All of the collected images were flattened to rule out any possible tilt.

Circular dichroism (CD) spectropolarimetry

HGFI-AR samples at a concentration of 50 μg/ml in MQW were used in this study, and the class I hydrophobin rHGFI was used as a positive control. The CD spectra of the assembled suspension were obtained after vigorously shaking on a vortex for 5 min to promote the formation of the β-sheet structure.

The spectra were recorded over the wavelength range from 190 to 250 nm on a Jasco J-715 CD spectrometer (Jasco, Japan), using a 1-mm quartz cuvette. The temperature was kept at 25 °C, and the sample compartment was continuously flushed with nitrogen gas. Samples' spectra are the result of averaging 5 scans obtained using a 5-s averaging per point, a bandwidth of 1 nm and a step width of 0.5 nm. The spectrum of the reference solution without the protein was used to correct for the background signal.

Thioflavin T (ThT) staining

All the samples used in the rodlet formation assays were tested using fluorescence emission spectroscopy. The samples were excited at 435 nm, and the emission spectra were recorded over the wavelength range of 450–600 nm with emission and excitation slits set at 10 nm. Lyophilized HGFI-AR and rHGFI were dissolved in MQW and added to a stock ThT solution prepared with MQW. The final concentrations in each sample were 5 μM ThT and 40 μg/mL HGFI-AR or rHGFI, respectively. The spectra were recorded using 5 μM ThT aqueous solution alone as a control. All the samples were measured using a Cary Eclipse Fluorescence Spectrophotometer (Varian Optical Spectroscopy Instruments, Mulgrave, Australia) before and after vortexing for 5 min.

Congo red (CR) binding assays

CR binding was performed using a BIO-TEK Microplate Reader model (BioTek U.S., Winooski, VT, USA); all measurements of the absorption spectra were recorded within a 300–700 nm range. The instrument was blanked using phosphate buffer (pH 4.0).

Both CR and the proteins were dissolved in 50 mM phosphate buffer (pH 4.0). Mixtures of CR and HGFI-AR or rHGFI were incubated at room temperature for 30 min

and shaked for 5 min prior to spectral analysis. The final concentrations in each sample consisted of 10 μg/ml CR and 100 μg/mL HGFI-AR or rHGFI, respectively. The absorbance spectra were also measured using 10 μg/ml CR solution alone as a control.

Results and discussion

Expression and purification of heterologously expressed HGFI-AR

A 80 bp gene *A1* and a 162 bp gene *A2* coding sequences were amplified by PCR using pET-28a-*hgfI* and pMD19-T-*hfbI* vectors, respectively, as templates. A 33-bp gene fragment encoding the amino acid sequence between Cys3 and Cys4 of HFBI was fused downstream of the gene *A1* and upstream of the gene *A2*. A 209 bp HGFI-AR coding sequence was obtained using the *A1* gene sequence and the *A2* fragment together as the template. The amplified HGFI-AR gene was inserted into the *P. pastoris* expression vector pPIC9 to construct the pPIC9-*hgfI-ar*. The corrected construction vector was identified by double enzymatic digestion with *Xho*I and *Eco*RI and DNA sequencing analysis. To ensure that the full-length HGFI-AR was secreted to the extracellular space without undesirable additional N-terminal amino acids, a Lys–Arg sequence specifically recognized and cleaved by the KEX2 protease was designed to be placed after the *Xho*I. The *hgfI-ar* gene was located downstream of the AOX1 promoter, which can be induced using methanol as sole carbon source (Burrowes et al. 2005).

The constructed plasmid pPIC9-*hgfI-ar* was linearized with *Stu*I, following its transfection into *P. pastoris* GS115 (His^-) cells using a Gene Pulser (Bio-Rad) apparatus (25 lF, 200 X, 2.0 kV) following the manufacturer's instructions. Fast-growing of the selected transformants (His^+Mut^+) was continued as described by Niu et al. (Niu et al. 2012a). After being selected on MD and MM media plates, fifteen fast-growing transformants (His^+ Mut^+) were chosen, identified by PCR and then sequencing using the primers 5′AOX/3′AOX.

Twelve positive transformants were induced in BMM with 0.5 % methanol at 28 °C for 96 h. The clone with the highest production of HGFI-AR was obtained after the supernatants of fermentation medium were analyzed by RP-HPLC. The purified HGFI-AR was obtained using a two-step procedure. The first step was ultrafiltration which was used to remove small impurities and concentrate the supernatant. Further purification was accomplished by RP-HPLC separation. The lyophilized HGFI-AR after ultrafiltration or RP-HPLC purification was analyzed on 16 % Tricine–SDS-PAGE. A clear band of about 6 kDa was found

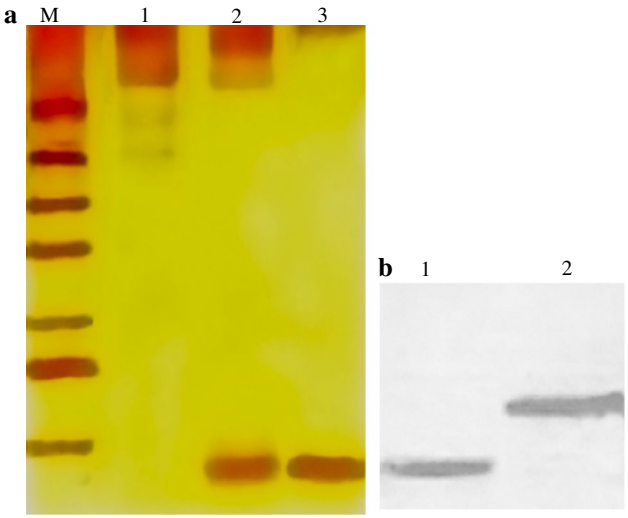

Fig. 1 **a** Silver-stained Tricine–SDS-PAGE of purified HGFI-AR expressed in *P. pastoris*. *M* molecular weight standards. *Lane 1* the lyophilisate from control strains. *Lane 2* the lyophilisate of HGFI-AR purified by ultrafiltration. *Lane 3* HGFI-AR purified by RP-HPLC; **b** Western blotting analysis of HGFI-AR using rHGFI as control. *Lane 1*, the purified HGFI-AR. *Lane 2* the purified rHGFI

in all transformants, which coincided with the expected HGFI-AR theoretical size, while the same band was absent in the control strains (*P. pastoris* transformed with pPIC9 vector) (Fig. 1a). The sequences of HGFI,HFBI and HGFI-AR are shown in Table 2. The purified protein HGFI-AR was analyzed by Western blotting using polyclonal anti-HGFI antibody, and the protein rHGFI was used as the positive control. The results showed that both proteins could specifically bind to the antibody (Fig. 1b).

To estimate the molecular weight of HGFI-AR precisely, the purified HGFI-AR protein was also analyzed with mass spectrometry. Its molecular weight was 5,989.43 Da. This value was less than the calculated molecular weight of 5,995.96 Da. This discrepancy may be attributed to the fact that the protein HGFI-AR is rich in cysteine residues and after its translation, intramolecular disulfide bonds could form which lead to the release of H^+ ions. The results mentioned above indicated that the heterologous protein was correctly folded in *P. pastoris* and also efficiently secreted from the cells without undesirable extra N-terminal amino acids.

WCA measurements

Wettability changes of the solid surfaces were probed before and after protein modification by WCA measurements (Fig. 2). The WCA of the bare polystyrene surface was 84.3 ± 2.5°. However, after self-assembling of HGFI-AR on the surface and rinsing with water, the WCA of the polystyrene surface was dramatically reduced

Table 2 The sequences of HGFI, HFBI and HGFI-AR

Hydrophobins	Sequence
HGFI	QQ**C**TTGQLQ**CC**ESTSTANDPATSELLGLIGVVISDVDALVGLT**C**SPISVIGVGSGSA**C**TANPV**CC**DSSPIG GLVSIG**C**VPVNV
HFBI	SNGNGNV**C**PPGLFSNPQ**CC**ATQVLGLIGLD**C**KVPSQNVYDGTDFRNV**C**AKTGAQPL**CC**VAPVAGQALL **C**QTAVGA
HGFI-AR	QQ**C**TTGQLQ**CC**ATQVLGLIGLD**C**SPISVIGVGSGSA**C**TANPV**CC**DSSPIGGLVSIG**C**VPVNV

The amino acids between third Cys and the fourth Cys of the class I hydrophobin HGFI from *G. frondosa* and of the class II hydrophobin HFBI from *T. reesei* are in underline. The conserved cysteine residues are in bold

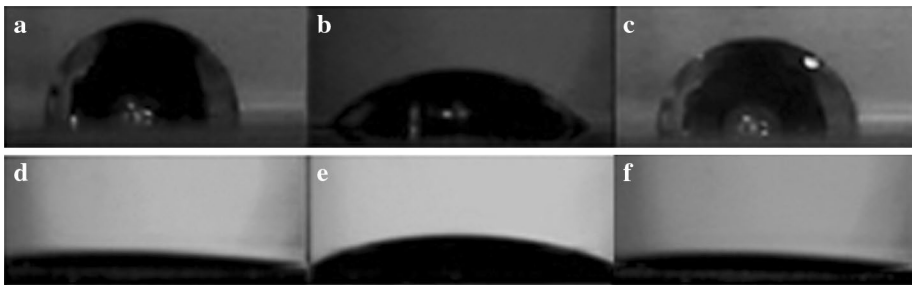

Fig. 2 WCA on **a** a bare polystyrene surface; **b** a HGFI-AR-modified polystyrene surface with water washing; **c** a HGFI-AR-modified polystyrene surface with SDS washing; **d** a native mica surface; **e** a HGFI-AR -modified mica surface with water washing; **f** a HGFI-AR-modified mica surface with SDS washing

to 37.3 ± 1.9°, this value was close to that of the rHGFI-coated polystyrene (Niu et al. 2012a). This result indicates that like class I hydrophobin rHGFI, the protein HGFI-AR could convert the surface of polystyrene from hydrophobic to hydrophilic. In comparison to the bare mica surface, the WCA value of HGFI-AR coated mica surface slightly increased from 6.4 ± 2.2° to 11.9 ± 1.7°, this result is also similar to that of the rHGFI-coated mica.

The presented results suggest that after the Cys3–Cys4 loop was replaced, HGFI-AR exhibited properties of amphipathic proteins that contained hydrophobic and hydrophilic patches. When HGFI-AR coats the hydrophobic polystyrene surface, a hydrophobic patch is induced by hydrophobic forces, and adsorbed onto the hydrophobic surface followed by the hydrophilic part which is exposed to the outside making the polystyrene surface hydrophilic. In turn, when HGFI-AR coats the hydrophilic mica surface, the hydrophilic patch is adsorbed onto the hydrophilic surface, leading to the exposure of the hydrophobic part to the outside making the mica surface hydrophobic.

To further investigate the resistance of the self-assembled film formed by HGFI-AR to be removed from polystyrene and mica surfaces, the HGFI-AR-coated polystyrene and mica surfaces were rinsed thoroughly with 1 % hot SDS. Unlike rHGFI and other class I hydrophobins, the WCA value of HGFI-AR coated polystyrene dramatically increased from 37.3 ± 1.9° to 82.3 ± 2.6°, this value is close to that of the bare polystyrene surface. Meanwhile, the WCA value of HGFI-AR coated mica surface was also close to that of the bare mica surface after washing with hot SDS.

An explanation for this behavior is provided as follows. First, after the Cys3–Cys4 fragment has been replaced, the number of hydrophobic amino acids was reduced from 14 to 6, which could lead to a decrease of interaction forces between HGFI-AR and polystyrene. The weaker membrane formed by HGFI-AR therefore becomes more susceptible to 1 % hot SDS washing. Second, in class I hydrophobins, the loop formed by the amino acids located between Cys3 and Cys4 plays a pivotal role in the rodlet structure formation and the self-assembly at hydrophilic–hydrophobic interface (Wang et al. 2004). When the number of amino acids between Cys3 and Cys4 is reduced from 32 to 11, the long disordered loop existing in class I hydrophobin HGFI may disappear which might result in losing self-assembly property that could form robust membranes at the polystyrene interface.

XPS measurements

The XPS survey spectra of the bare and HGFI-AR-modified siliconized glass are shown in Fig. 3. The relative elemental composition of the bare and HGFI-AR-modified siliconized glass is shown in Table 3.

In the spectrum of bare siliconized glass, a high intensity of O 1*s* and Si 2*p* signals and a low intensity of C 1*s* signal

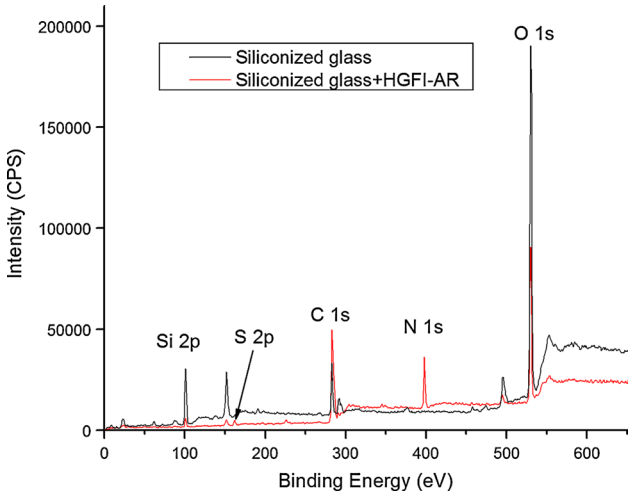

Fig. 3 XPS spectra of siliconized glass surfaces before and after HGFI-AR modification

were detected, which is typical of the bare siliconized glass composition. In addition, and as expected, the N 1*s* and S 2*p* signals were not observed. After HGFI-AR modification and water rinsing, the elemental composition significantly changed. The intensity of the Si 2*p* peak dramatically decreased, and the C 1*s* and N 1*s* signals became predominant. In addition, a high intensity of N 1*s* and a weak intensity of S 2*p* were detected. Obviously, there is no Si element in the protein HGFI-AR, it only existed in the siliconized glass, but the elements N and S only correlate to the presence of the protein. Therefore, HGFI-AR showed a similar behavior as the class I hydrophobin rHGFI (Wang et al. 2010a), which could form a robust membrane on solid surfaces and tolerate rinsing with water.

Yet, the phenomena above described were limited to the treatment that only involved a water wash. When the HGFI-AR-modified siliconized glass was washed with 1 % hot SDS, the elemental composition reverted back to the bare siliconized glass (data not shown). This meant that the robust membrane formed by HGFI-AR on siliconized glass surface did not resist the hot SDS wash. The result of the XPS measurements also supported the conclusion we obtained from the WCA measurements that Cys3–Cys4 of class I hydrophobin HGFI played an important role when self-assembled at hydrophilic/hydrophobic interfaces.

Atomic force microscope measurements

When a droplet of HGFI-AR solution was placed on a freshly cleaved mica surface, the formation of a distinctive monolayer of protein was clearly observed (Fig. 4a). This hydrophobin film seemed to be compact, except for some irregular holes embedded in it. Moreover, no rodlet structure was observed.

While, typical rodlet structures were visualized when rHGFI solution was dried on a freshly cleaved mica surface (Fig. 4b). Like the native HGFI, most of the rodlets that rHGFI formed were about 100 nm in length and extended in different directions.

According to the previous studies, the characteristic rodlet structure only was present in class I hydrophobins, and it was also a key difference between class I and class II hydrophobins (Linder et al. 2005; Linder 2009). So, it can be speculated that the amino acids between Cys3 and Cys4

Table 3 The relative elemental compositions of the bare and HGFI-AR modified siliconized glass surfaces

Spectra sample	C 1 *s* (%)	N 1 *s* (%)	O 1 *s* (%)	Si 2*p* (%)	S 2*p* (%)
Siliconized glass	8.96	0.90	55.34	22.50	0.00
Siliconized glass + rHGFI-AR	55.89	12.06	28.10	3.18	0.77

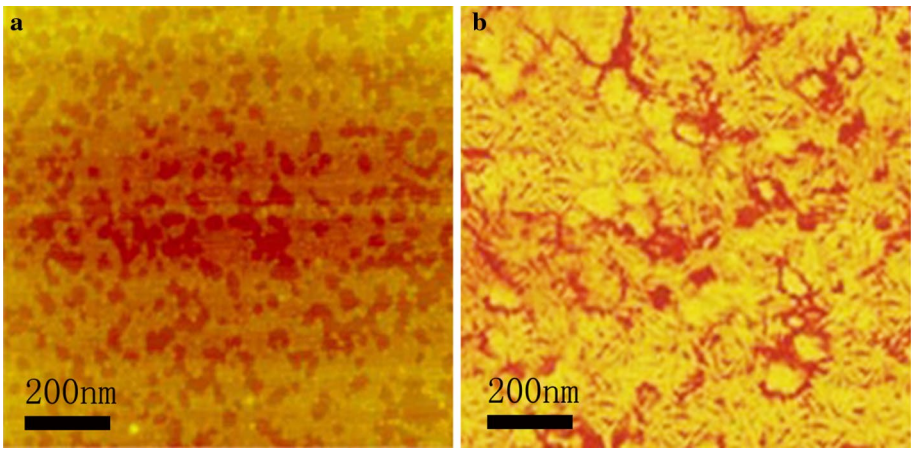

Fig. 4 AFM images of different hydrophobins dried onto mica, image size is 1 × 1 μm and height scale is 10 nm. **a** HGFI-AR; **b** rHGFI

of HGFI play a decisive role in the rodlet structure forming process of class I hydrophobin HGFI. This result differs from the data that the Cys3–Cys4 loop of Hydrophobin EAS was not required for rodlet formation (Kwan et al. 2008). Although there is no clear explanation for the discrepancy of our results from previous studies, it might be attributed to the following: First, the number and composition of amino acids between HGFI and EAS are fairly different. Second, the process used to obtain the mutant protein HGFI-AR is different for truncated versions of class I hydrophobin EAS (Wessels 1994; de Vries et al. 1999).

Secondary structure changes upon self-assembly of HGFI-AR and HGFI

CD spectroscopy was used to study the secondary structural changes of HGFI-AR and rHGFI between their monomeric and self-assembled forms at the water–air interface. CD spectra of the monomeric HGFI-AR in water showed a maximum ellipticity close to 190 nm and a minimum close to 205 nm (Fig. 5a, thick line). After vigorous shaking, the CD spectra were similar to that of the original HGFI-AR aqueous solution, except for a slight decrease in the intensity of the spectrum. CD spectra of the rHGFI in water had a maximum ellipticity close to 190 nm and a minimum close to 205 nm (Fig. 5a, dotted line). Contrary to HGFI-AR, great changes were observed in the CD spectra of rHGFI after vigorous shaking of the solutions (Fig. 5b). It is presumed that the assemblages acquire a predominately β-sheet structure indicated by the minima shifted from 205 to 215–217 nm, which is the same as the value found from all other class I hydrophobins studied to this date (Askolin et al. 2006; Ma et al. 2008; Janssen et al. 2004; De Vocht et al. 2002).

The lack of structural changes observed after HGFI-AR self-assembled at the water–air interface might be explained as follows. After the Cys3–Cys4 of HGFI was replaced, the number of hydrophobic amino acid decreased which led to a reduction in the hydrophobic interaction between hydrophobins/hydrophobins and hydrophobins/air bubbles. Therefore, when the assemblages of HGFI-AR were formed at water–air interface, their inherent instability precluded any structural change.

Self-assembly and surface activity of the HGFI-AR

ThT is known to greatly increase its fluorescence yield upon binding to stacked β-sheets (LeVine Iii 1999) and Congo red (CR) exhibits a significant shift in its absorption spectrum in the presence of stacked β-sheets (Klunk et al. 1999). So, to identify whether the purified HGFI-AR retained the ability to self-assemble into amyloid-like structures as class I hydrophobins, CR and ThT-binding assays were performed as described in the Materials and methods

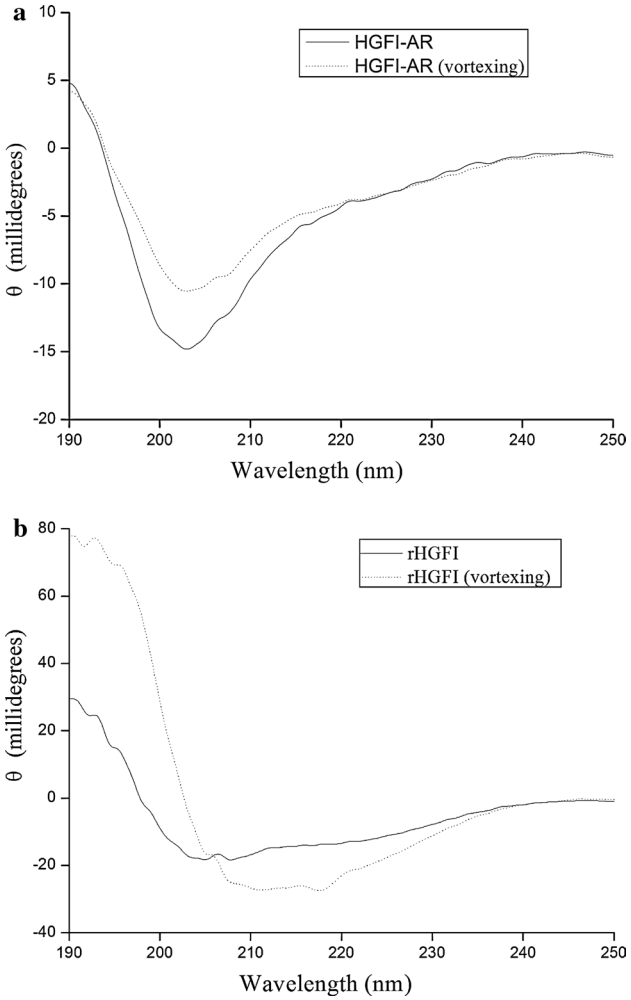

Fig. 5 CD spectra of the mutant protein HGFI-AR (**a**) and the class I hydrophobin rHGFI (**b**) in water (*thick line*) and after vigorous shaking (*dotted line*). CD spectra were the averages of 5 scans

section. The maximum fluorescence intensity of ThT and hydrophobin–ThT mixed solution was observed at 485 nm before and after vortexing for 5 min (Fig. 6).

The fluorescence intensity of ThT and rHGFI mixed solution was twofold higher than that of pure ThT water solution before vortexing. Progressively this difference became more pronounced reaching a 4.5-fold after vortexing (Fig. 6a). This phenomenon correlates well with the results obtained during the study of some other class I hydrophobins (Stroud et al. 2003; Macindoe et al. 2012). When compared to rHGFI, no significant increase in the fluorescence intensity of ThT/HGFI-AR solutions was observed after vortexing (Fig. 6b). The maximum fluorescence intensities of HGFI-AR/THT mixed solutions at 485 nm were tested after vortexing for 10, 20, 30 and 40 min in different pH (3, 5, 7, 9). There was also no significant increase in the fluorescence intensity of ThT/HGFI-AR solutions observed after vortexing.

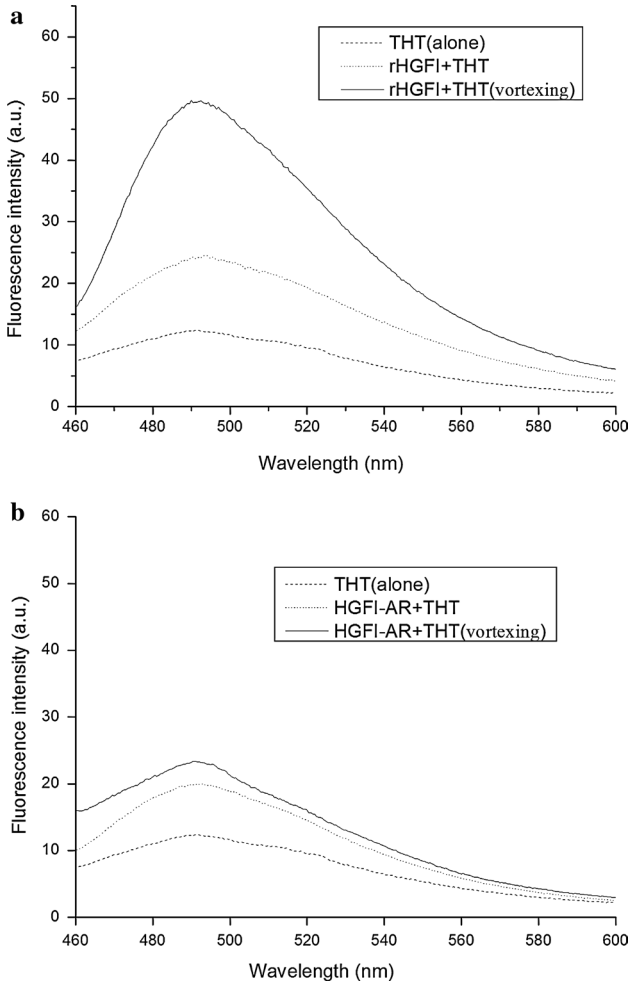

Fig. 6 Fluorescence emission spectra of thioflavin T in the presence of rHGFI or HGFI-AR. **a** The sample contained ThT alone (*dashed line*) or in the presence of unvortexed (*dotted line*) or vortexed (*solid line*) rHGFI; **b** The sample contained ThT alone (*dashed line*) or in the presence of unvortexed (*dotted line*) or vortexed (*solid line*) HGFI-AR

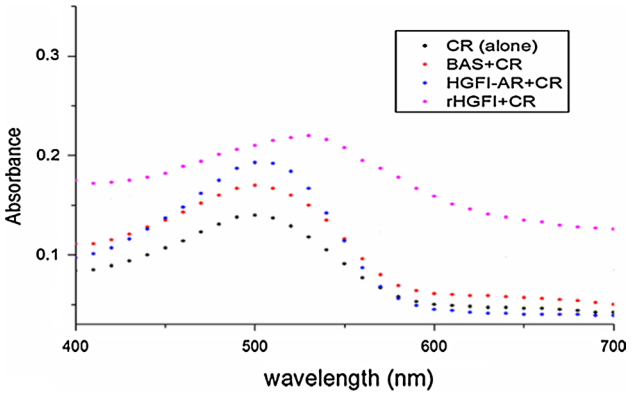

Fig. 7 The adsorption spectra of different Congo red solutions

Similar to ThT, CR can also bind to ordered stacks of β-sheets and cause absorption spectra shifts. Although the details of the interaction between the two dyes and stacked β- sheets have not been yet elucidated, in principle it can be speculated that the two dyes may not bind to the same sites on proteins due to their opposite charges.

Since both the hydrophobins and CR are negatively charged at neutral pH, the existing electrostatic repulsion may prevent the binding from happening. Therefore, to avoid repulsion, the CR assay was performed at a lower pH (4.0). The spectra of protein/CR and CR alone are shown in Fig. 7. BSA was used as a negative control since this protein only presents a limited extent of β-structure. Contrary to CR, rHGFI/CR showed a spectrum shift from 490 to 530 nm. It should also be noticed that no appreciable difference in spectra was observed from HGFI-AR and BSA.

The higher fluorescence intensity of ThT in mixed protein solutions without vortexing indicated that both rHGFI and HGFI-AR might contain some stacked β-sheets even in the monomeric structure or that the protein solutions were not completely monomeric before the assay. The increased fluorescence intensity was hardly detected in HGFI-AR mixed solution after vortexing. In this case, it can be hypothesized that unstable or no amyloid-like structures were formed. Although further studies should be conducted to explain why HGFI-AR did not cause a fluorescence intensity increase and a CR absorption spectrum shift, protease digestion and hydrogen–deuterium exchange studies could contribute to explain these observations (Wang et al. 2004). They had already indicated that the second loop of class I hydrophobin SC3 plays a pivotal role in self-assembly at hydrophilic–hydrophobic interface.

From the comparison of sequence alignment between class I and II hydrophobins, we know that in class I hydrophobins, the segment of amino acids between Cys3 and Cys4 is the least conserved portion in terms of size and make-up. In addition, the loop formed by them is largely disordered and extremely hydrophobic. Of interest, this loop formed by the corresponding amino acids in class II hydrophobins is much smaller, conserved (11 residues between Cys3 and Cys4) and binds less tightly to hydrophobic surfaces.

Therefore, a noticeable change in functionality and behavior was expected in the class I hydrophobin HGFI structure after the 32 residues between Cys3 and Cys4 were replaced by 11 residues between Cys3 and Cys4 of class II hydrophobin HFBI. The replacement might lead HGFI-AR to acquire properties of class II hydrophobins as shown in the above reported studies. In addition, in our research both rodlet formation and surface activity were modified after the residues were replaced. The nature of the alterations differed from the results reported using another class I hydrophobin EAS (Kwan et al. 2008). Although, there is

little amino acid sequence homology in class I and class II hydrophobins, they share very similar folds, which have almost identical β-barrel folds that are composed of four antiparallel β-strands (Sunde et al. 2008; Zampieri et al. 2010). When the three-dimensional structure of class I and class II hydrophobin formed, the disordered Cys3–Cys4 loop of the class I hydrophobin EAS was on the protein surface. In contrast, the Cys3–Cys4 loop of the class II hydrophobin HFBI was located inside (Zampieri et al. 2010). So, after deletion of the residues from Cys3–Cys4 loop of the class I hydrophobin EAS, the rest of the residues of this loop might be still on EAS surface, which could facilitate the rodlet formation of EAS. While, after the Cys3–Cys4 fragment has been replaced, the Cys3–Cys4 loop of HGFI-AR might be located inside, which led to that HGFI-AR could not form rodlet structures.

Conclusions

In this work, a mutant protein HGFI-AR was obtained by replacing the amino acids between Cys3 and Cys4 of class I hydrophobin HGFI from *Grifola frondosa* with those ones between Cys3 and Cys4 of class II hydrophobin HFBI from *Trichoderma reesei*. The gene of HGFI-AR was successfully expressed in methylotrophic yeast *P. pastoris* GS115.

We have demonstrated that like the native hydrophobins, the mutant protein HGFI-AR could form amphipathic membranes at different surfaces to alter their wettabilities. In comparison to rHGFI, the film formed by HGFI-AR at a hydrophobic surface was less stable. Moreover, the self-assembly of HGFI-AR at the water–air interface was not accompanied with a increase of β-sheet conformational change in secondary structure, and no typical rodlet structure was observed after HGFI-AR coating on solid surfaces. Thus, it could be speculated that the Cys3–Cys4 loop in HGFI plays an important role in its conformation and functionality, when HGFI self-assembles at hydrophobic–hydrophilic interfaces.

Acknowledgments This research was financially supported by the National Natural Science Foundation of China (31170066), Tianjin Key Research Program of Application Foundation and Advanced Technology (12JCZDJC22600) and the Natural Science Foundation of Shanxi Province (2014021020-3).

Conflict of interest The authors declare that they have no conflict of interest.

References

Askolin S, Linder M, Scholtmeijer K, Tenkanen M, Penttilä M, de Vocht ML, Wösten HAB (2006) Interaction and comparison of a class I hydrophobin from Schizophyllum commune and class II hydrophobins from *Trichoderma reesei*. Biomacromolecules 7(4):1295–1301. doi:10.1021/bm050676s

Basheva ES, Kralchevsky PA, Danov KD, Stoyanov SD, Blijdenstein TBJ, Pelan EG, Lips A (2011) Self-assembled bilayers from the protein HFBII hydrophobin: nature of the adhesion energy. Langmuir 27(8):4481–4488. doi:10.1021/la2001943

Burrowes O-J, Diamond G, Lee T-C (2005) Recombinant expression of pleurocidin cDNA using the *Pichia pastoris* expression system. J Biomed Biotechnol 4:374–384. doi:10.1155/jbb.2005.374

Butko P, Buford JP, Goodwin JS, Stroud PA, McCormick CL, Cannon GC (2001) Spectroscopic evidence for amyloid-like interfacial self-assembly of hydrophobin Sc3. Biochem Biophys Res Commun 280(1):212–215. doi:10.1006/bbrc.2000.4098

de Vocht ML, Scholtmeijer K, van der Vegte EW, de Vries OMH, Sonveaux N, Wösten HAB, Ruysschaert J-M, Hadziioannou G, Wessels JGH, Robillard GT (1998) Structural characterization of the hydrophobin SC3, as a monomer and after self-assembly at hydrophobic/hydrophilic interfaces. Biophys J 74(4):2059–2068. doi:10.1016/S0006-3495(98)77912-3

De Vocht ML, Reviakine I, Ulrich W-P, Bergsma-Schutter W, Wösten HAB, Vogel H, Brisson A, Wessels JGH, Robillard GT (2002) Self-assembly of the hydrophobin SC3 proceeds via two structural intermediates. Protein Sci 11(5):1199–1205. doi:10.1110/ps.4540102

de Vries OMH, Moore S, Arntz C, Wessels JGH, Tudzynski P (1999) Identification and characterization of a tri-partite hydrophobin from *Claviceps fusiformis*. Eur J Biochem 262(2):377–385. doi:10.1046/j.1432-1327.1999.00387.x

Hakanpää J, Paananen A, Askolin S, Nakari-Setälä T, Parkkinen T, Penttilä M, Linder MB, Rouvinen J (2004) Atomic resolution structure of the HFBII hydrophobin, a self-assembling amphiphile. J Biol Chem 279(1):534–539. doi:10.1074/jbc.M309650200

Hakanpää J, Linder M, Popov A, Schmidt A, Rouvinen J (2006) Hydrophobin HFBII in detail: ultrahigh-resolution structure at 0.75 A. Acta Crystallogr Sect D 62(4):356–367. doi:10.1107/S0907444906000862

Hou S, Li X, Li X, Feng X-Z, Wang R, Wang C, Yu L, Qiao M-Q (2009) Surface modification using a novel type I hydrophobin HGFI. Anal Bioanal Chem 394(3):783–789. doi:10.1007/s00216-009-2776-y

Houmadi S, Ciuchi F, De Santo MP, De Stefano L, Rea I, Giardina P, Armenante A, Lacaze E, Giocondo M (2008) Langmuir–Blodgett film of hydrophobin protein from *Pleurotus ostreatus* at the air–water interface. Langmuir 24(22):12953–12957. doi:10.1021/la802306r

Janssen MI, Leeuwen MBMv, Kooten TGv, Vries Jd, Dijkhuizen L, Wösten HAB (2004) Promotion of fibroblast activity by coating with hydrophobins in the β-sheet end state. Biomaterials 25(14):2731–2739. doi:10.1016/j.biomaterials.2003.09.060

Kershaw MJ, Talbot NJ (1998) Hydrophobins and repellents: proteins with fundamental roles in fungal morphogenesis. Fungal Genet Biol 23(1):18–33. doi:10.1006/fgbi.1997.1022

Klunk WE, Jacob RF, Mason RP (1999) Quantifying amyloid by congo red spectral shift assay. In: Ronald W (ed) Methods in enzymology, vol 309. Academic Press, New York, pp 285–305. doi:10.1016/S0076-6879(99)09021-7

Kwan AHY, Winefield RD, Sunde M, Matthews JM, Haverkamp RG, Templeton MD, Mackay JP (2006) Structural basis for rodlet assembly in fungal hydrophobins. Proc Natl Acad Sci USA 103(10):3621–3626. doi:10.1073/pnas.0505704103

Kwan AH, Macindoe I, Vukašin PV, Morris VK, Kass I, Gupte R, Mark AE, Templeton MD, Mackay JP, Sunde M (2008) The Cys3–Cys4 loop of the hydrophobin EAS is not required for rodlet formation and surface activity. J Mol Biol 382(3):708–720. doi:10.1016/j.jmb.2008.07.034

LeVine Iii H (1999) Quantification of β-sheet amyloid fibril structures with thioflavin T. In: Ronald W (ed) Methods in enzymology, vol 309. Academic Press, New York, pp 274–284. doi:10.1016/S0076-6879(99)09020-5

Linder MB (2009) Hydrophobins: proteins that self assemble at interfaces. Curr Opin Colloid Interf Sci 14(5):356–363. doi:10.1016/j.cocis.2009.04.001

Linder MB, Szilvay GR, Nakari-Setälä T, Penttilä ME (2005) Hydrophobins: the protein-amphiphiles of filamentous fungi. FEMS Microbiol Rev 29(5):877–896. doi:10.1016/j.femsre.2005.01.004

Lugones LG, Wösten HAB, Wessels JGH (1998) A hydrophobin (ABH3) specifically secreted by vegetatively growing hyphae of *Agaricus bisporus* (common white button mushroom). Microbiology 144(8):2345–2353. doi:10.1099/00221287-144-8-2345

Ma H, Snook LA, Tian C, Kaminskyj SGW, Dahms TES (2006) Fungal surface remodelling visualized by atomic force microscopy. Mycol Res 110(8):879–886. doi:10.1016/j.mycres.2006.06.010

Ma A, Shan L, Wang H, Du Z, Xie B (2008) Partial characterization of a hydrophobin protein Po.HYD1 purified from the oyster mushroom *Pleurotus ostreatus*. World J Microbiol Biotechnol 24(4):501–507. doi:10.1007/s11274-007-9500-x

Macindoe I, Kwan AH, Ren Q, Morris VK, Yang W, Mackay JP, Sunde M (2012) Self-assembly of functional, amphipathic amyloid monolayers by the fungal hydrophobin EAS. Proc Natl Acad Sci USA. doi:10.1073/pnas.1114052109

Morris VK, Ren Q, Macindoe I, Kwan AH, Byrne N, Sunde M (2011) Recruitment of class I hydrophobins to the air:water interface initiates a multi-step process of functional amyloid formation. J Biol Chem 286(18):15955–15963. doi:10.1074/jbc.M110.214197

Niu B, Huang Y, Zhang S, Wang D, Xu H, Kong D, Qiao M (2012a) Expression and characterization of hydrophobin HGFI fused with the cell-specific peptide TPS in *Pichia pastoris*. Protein Express Purif 83(1):92–97. doi:10.1016/j.pep.2012.03.004

Niu B, Wang D, Yang Y, Xu H, Qiao M (2012b) Heterologous expression and characterization of the hydrophobin HFBI in *Pichia pastoris* and evaluation of its contribution to the food industry. Amino Acids 43(2):763–771. doi:10.1007/s00726-011-1126-5

Paananen A, Vuorimaa E, Torkkeli M, Penttilä M, Kauranen M, Ikkala O, Lemmetyinen H, Serimaa R, Linder MB (2003) Structural hierarchy in molecular films of two class II hydrophobins. Biochemistry 42(18):5253–5258. doi:10.1021/bi034031t

Paslay LC, Falgout L, Savin DA, Heinhorst S, Cannon GC, Morgan SE (2013) Kinetics and control of self-assembly of ABH1 hydrophobin from the edible White Button mushroom. Biomacromolecules 14(7):2283–2293. doi:10.1021/bm400407c

Sbrana F, Fanelli D, Vassalli M, Carresi L, Scala A, Pazzagli L, Cappugi G, Tiribilli B (2010) Progressive pearl necklace collapse mechanism for cerato-ulmin aggregation film. Eur Biophys J 39(6):971–977. doi:10.1007/s00249-009-0465-6

Scholtmeijer K, Wessels J, Wösten H (2001) Fungal hydrophobins in medical and technical applications. Appl Microbiol Biotechnol 56(1–2):1–8. doi:10.1007/s002530100632

Serimaa R, Torkkeli M, Paananen A, Linder M, Kisko K, Knaapila M, Ikkala O, Vuorimaa E, Lemmetyinen H, Seeck O (2003) Self-assembled structures of hydrophobins HFBI and HFBII. J Appl Crystallogr 36(3 Part 1):499–502. doi:doi:10.1107/S0021889803000578

Stroud PA, Goodwin JS, Butko P, Cannon GC, McCormick CL (2003) Experimental evidence for multiple assembled states of Sc3 from Schizophyllum commune. Biomacromolecules 4(4):956–967. doi:10.1021/bm034045e

Sunde M, Kwan AHY, Templeton MD, Beever RE, Mackay JP (2008) Structural analysis of hydrophobins. Micron 39(7):773–784. doi:10.1016/j.micron.2007.08.003

Talbot NJ, Kershaw MJ, Wakley GE, De Vries O, Wessels J, Hamer JE (1996) MPG1 encodes a fungal hydrophobin involved in surface interactions during infection-related development of *Magnaporthe grisea*. Plant Cell Online 8(6):985–999. doi:10.1105/tpc.8.6.985

Trembley ML, Ringli C, Honegger R (2002) Hydrophobins DGH1, DGH2, and DGH3 in the lichen-forming basidiomycete *Dictyonema glabratum*. Fungal Genet Biol 35(3):247–259. doi:10.1006/fgbi.2001.1325

Wang X, Permentier HP, Rink R, Kruijtzer JAW, Liskamp RMJ, Wösten HAB, Poolman B, Robillard GT (2004) Probing the self-assembly and the accompanying structural changes of hydrophobin SC3 on a hydrophobic surface by mass spectrometry. Biophys J 87(3):1919–1928

Wang Z, Feng S, Huang Y, Li S, Xu H, Zhang X, Bai Y, Qiao M (2010a) Expression and characterization of a *Grifola frondosa* hydrophobin in *Pichia pastoris*. Protein Express Purif 72(1):19–25. doi:10.1016/j.pep.2010.03.017

Wang Z, Huang Y, Li S, Xu H, Linder MB, Qiao M (2010b) Hydrophilic modification of polystyrene with hydrophobin for time-resolved immunofluorometric assay. Biosensors Bioelectron 26(3):1074–1079. doi:10.1016/j.bios.2010.08.059

Wessels JGH (1994) Developmental regulation of fungal cell wall formation. Annu Rev Phytopathol 32(1):413–437. doi:10.1146/annurev.py.32.090194.002213

Wessels JGH (1996) Hydrophobins: proteins that change the nature of the fungal surface. Adv Microb Physiol 38. doi:10.1016/s0065-2911(08)60154-x

Wessels J, De Vries O, Asgeirsdottir SA, Schuren F (1991) Hydrophobin genes involved in formation of aerial hyphae and fruit bodies in Schizophyllum. Plant Cell Online 3(8):793–799. doi:10.1105/tpc.3.8.793

Wösten HAB (2001) Hydrophobins: multipurpose proteins. Annu Rev Microbiol 55(1):625–646. doi:10.1146/annurev.micro.55.1.625

Wösten HAB, de Vocht ML (2000) Hydrophobins, the fungal coat unravelled. Biochim Biophys Acta Rev Biomembr 1469(2):79–86. doi:10.1016/S0304-4157(00)00002-2

Wösten HAB, Wessels JGH (1997) Hydrophobins, from molecular structure to multiple functions in fungal development. Mycoscience 38(3):363–374. doi:10.1007/bf02464099

Wösten HAB, van Wetter M-A, Lugones LG, van der Mei HC, Busscher HJ, Wessels JGH (1999) How a fungus escapes the water to grow into the air. Curr Biol 9(2):85–88. doi:10.1016/S0960-9822(99)80019-0

Yang W, Ren Q, Wu Y-N, Morris VK, Rey AA, Braet F, Kwan AH, Sunde M (2013) Surface functionalization of carbon nanomaterials by self-assembling hydrophobin proteins. Biopolymers 99(1):84–94. doi:10.1002/bip.22146

Yu L, Zhang B, Szilvay GR, Sun R, Jänis J, Wang Z, Feng S, Xu H, Linder MB, Qiao M (2008) Protein HGFI from the edible mushroom *Grifola frondosa* is a novel 8 kDa class I hydrophobin that forms rodlets in compressed monolayers. Microbiology 154(6):1677–1685. doi:10.1099/mic.0.2007/015263-0

Zampieri F, Wösten HAB, Scholtmeijer K (2010) Creating surface properties using a palette of hydrophobins. Materials 3:4607–4625. doi:10.3390/ma3094607